

https://doi.org/10.1070/QEL16798

Simultaneous mode locking and *Q*-switching in a solid-state laser with a travelling-wave acousto-optic modulator and retroreflector

O.E. Nanii, A.I. Odintsov, A.I. Panakov, A.P. Smirnov, A.I. Fedoseev

Abstract. **This paper presents a numerical study of the dynamics of a mode-locked, *Q*-switched laser whose cavity contains a travelling-wave acousto-optic modulator (AOM) and a retroreflector which returns the zeroth- and first-order diffracted waves to the AOM. The reflectivity of the retroreflector depends on the order of diffraction. If the AOM is switched on once or periodically, lasing is characterised by a pulse train frequency sweep. Keeping the AOM constantly switched on leads to self-oscillations. Their characteristics can be controlled by varying the detuning of the operating frequency of the modulator from resonance.**

Keywords: *laser, mode locking, Q-switching, acousto-optic modulator, self-oscillations.*

1. Introduction

Solid-state lasers that are both *Q*-switched and mode-locked (QML lasers) allow one to obtain trains of high-peak-power, short optical pulses. Owing to this, they have found application in high-precision materials processing, optical tomography, time-resolved spectroscopy, measuring tools and other areas [1–3].

Passive *Q*-switching methods (e. g. using saturable absorbers) ensure QML laser operation [4, 5]. The insufficient stability of emission parameters which is inherent in passive methods has been obviated in more complex configurations [6, 7], in which the repetition rate of pulse trains is controlled by an active *Q*-switch and the formation of mode-locked (ML) pulses in a train is ensured by a combination of passive and active *Q*-switching.

The most promising QML laser configurations are those in which both *Q*-switching and mode locking are brought about by a single device: travelling-wave acousto-optic modulator (AOM). In such QML lasers, the AOM ensures that both the undiffracted wave (zeroth order) and the doubly first-order diffracted wave (whose frequency is hence shifted by $2f$, where f is the operating frequency of the modulator) return to the cavity. To achieve mode locking, f should be about half the mode spacing. For effective experimental implementation of this approach, Donin et al. [8, 9] used a spherical mirror and placed an AOM at its focus.

According to a numerical model proposed previously for the QML laser [10], the diffraction coefficient is a governing parameter that can radically change the dynamics of the system. In particular, it is shown that, in a rather wide range of parameters of a system, self-oscillations in the form of periodic trains of short ML pulses are possible.

In this paper, using a modified numerical model we consider a laser in which a retroreflector is used to return the transmitted and diffracted beams. One configuration of such a device is schematised in Fig. 1. The mirrors of the retroreflector are independent [11], and their reflectivity for the first order of diffraction (r_2) far exceeds that for the zeroth order (r_1). To reduce the sensitivity of the system to mechanical stimuli, a diffraction grating with a relatively low spectral resolution (a relatively small number of grating lines) can be used instead of mirrors. The plane of the grating corresponds to the plane of the mirror for reflecting the zeroth diffraction order in the AOM, and the plane of a line corresponds to the plane of the mirror for reflecting the diffracted wave. It is also possible to use a single spherical mirror whose reflectivity depends on one coordinate.

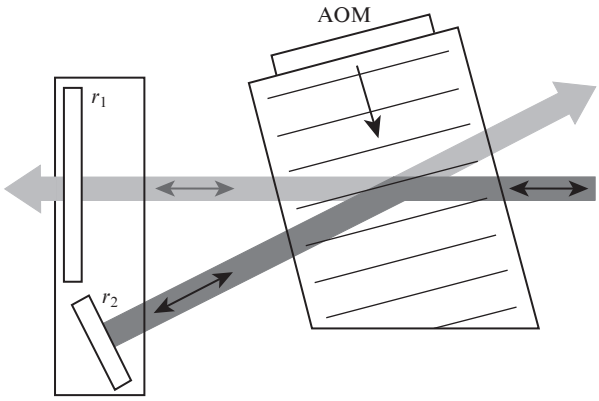

Figure 1. Optical scheme comprising an AOM and retroreflector.

2. Model

The model builds on a modal approach based on balance equations [10]. In this work, not only the distinctive feature due to the optical scheme but also the stochastic field of spontaneous emission are taken into account, as was done by Kasahara et al. [12] and Stellpflug et al. [13] for describing a

O.E. Nanii, A.I. Odintsov, A.I. Panakov, A.I. Fedoseev Faculty of Physics, M.V. Lomonosov Moscow State University, Vorob'evy gory, 119991 Moscow, Russia; e-mail: naniy@t8.ru;
A.P. Smirnov Faculty of Computational Mathematics and Cybernetics, M.V. Lomonosov Moscow State University, Vorob'evy gory, 119991 Moscow, Russia

Received 3 August 2018; revision received 18 October 2018
Kvantovaya Elektronika **49** (2) 119–123 (2019)
Translated by O.M. Tsarev

'modeless' laser. As above, a condition for an exact (resonance) tuning of the operating frequency of the AOM, f, to the mode spacing frequency is $f = \delta\nu_c/2$ (where $\delta\nu_c$ is the mode spacing). In all calculations, we take into account the nonzero detuning $\delta\nu$ from the resonance frequency ($\delta\nu = \delta\nu_c - 2f$).

Equations for the normalised field amplitudes E_j with allowance for their phases φ_j have the following form (in the case of the $j = 0$ mode, there is no second term):

$$\frac{\mathrm{d}}{\mathrm{d}\tau}E_j\exp(\mathrm{i}\varphi_j) = \left[\mu_1\left(\frac{\sigma_j}{\sigma_0}n - 1\right) - \gamma\right]E_j\exp(\mathrm{i}\varphi_j) + \left[\mu_2\left(\frac{\sigma_j}{\sigma_0}n - \frac{\theta_2}{\theta_1}\right)\right]\kappa_\mathrm{d}^2E_{j-1}\exp[\mathrm{i}(\varphi_{j-1} + 2\pi\frac{\delta\nu}{\delta\nu_c}\tau)] + \mu_3 nE_j^{\mathrm{sp}}\exp(\mathrm{i}\varphi_{\mathrm{sp}}). \quad (1)$$

Here, time τ is normalised to the cavity round-trip time $T_c = 2L/c$ (where L is the separation between the mirrors), and inversion n is normalised to the cavity loss $\theta_1 = |\ln r_1|$. The ratio of the transition cross sections, σ_j/σ_0, takes into account the decrease in gain with increasing distance from the centre of a homogeneously broadened line (at $j = 0$): $\sigma_j/\sigma_0 = (1 + j^2b^2)^{-1}$, $b = \delta\nu_c/\delta\nu_g$, where $\delta\nu_g$ is the gain linewidth. The parameter $\mu_1 = cT_c\theta_1/2L$ determines the rate of field attenuation in the cavity with no allowance for the diffraction loss. The analogous quantity for the loop containing the diffracted beam can be written as $\mu_2 = cT_c\theta_2/2L$ ($\theta_2 = |\ln r_2|$ is the loss due to the incomplete reflection in the loop); $\mu_3 = T_c/T_1$ (where T_1 is the inversion relaxation time). The loss due to diffraction in the cavity has the form $\gamma = -\ln(1 - \kappa_\mathrm{d}^2)$, where κ_d is the diffraction coupling coefficient (the fraction of the optical field reflected from the acoustic wave in the AOM). The spontaneous field of each mode is $E_j^{\mathrm{sp}} = E_{\mathrm{sp}}\sigma_j/\sigma_0$. We assume that the E_{sp} of each mode varies randomly between zero and its maximum value and that the phase φ_{sp} varies independently and also randomly from 0 to 2π in a time equal to the inverse of the gain linewidth. The total intensity I as a function of time τ can be calculated as the absolute square of the sum of the complex mode fields:

$$I(\tau) = \left|\sum_j E_j\exp[\mathrm{i}\psi_j(\tau)]\right|^2, \quad (2)$$

where $\psi_j(\tau) = j2\pi\tau + \varphi_j$. Saturation of the medium is thought to be approximately determined by the sum of the average mode intensities:

$$\bar{I}(\tau) = \sum_j |E_j|^2\frac{\sigma_j}{\sigma_0}.$$

The balance equation for inversion n has the form

$$\frac{\mathrm{d}}{\mathrm{d}\tau}n = \frac{T_c}{T_1}\left[\eta - n\left(1 + \sum_j |E_j|^2\frac{\sigma_j}{\sigma_0}\right)\right]. \quad (3)$$

Here, η is the pump parameter (the ratio of the pump rate to its threshold in the cavity in the absence of diffraction). The field amplitudes E_j in (1)–(3) are normalised to $\sqrt{I_0}$, where I_0 is the steady-state intensity of the fundamental mode at $\eta = 2$.

In most computations, the following parameters were used: $r_1 = 0.1$, $r_2 = 0.9$, $T_1 = 2.5\times10^{-4}$ s, $\delta\nu_c = 100$ MHz, $\delta\nu_g = 100$ GHz and $\eta = 4$. The maximum field of spontaneous emission to each mode E_{sp} was estimated at 10^{-8}. The computations took into account up to 300 modes. High-order modes whose fields were lower than the spontaneous emission level throughout the computation time were left out of account.

3. External Q-switching regime

In the case of external Q-switching, initial conditions correspond to steady-state lasing with the AOM switched off. The laser operates only on the central mode with $j = 0$. The steady-state lasing parameters are $E_0 = \sqrt{\eta - 1}$ and $n = 1$.

After the AOM is switched on, doubly diffracted light appears in the cavity, which experiences markedly lower losses because the reflectivity r_2 considerably exceeds r_1. This results in Q-switching, which shows up most clearly at a relatively high value of κ_d (0.4–0.8). In the system under consideration, this effect has a feature related to field injection into the next mode. Figure 2 shows the changes in mode intensities immediately after the AOM was instantaneously switched on (here and in what follows, the intensity of mode j is $I_j = |E_j|^2$). The intensity of the $j = 0$ mode rapidly drops to zero, which is accompanied by a sequential increase in the intensity of each subsequent mode (Fig. 2, inset). Since the increase is predominantly due to the drop in the intensity of the preceding mode, the intensity of each mode has the form of a pulse which reaches the highest intensity at a time τ close to the number of the mode j. With decreasing inversion, the increase in pulse intensity I_j gives way to a decrease, so the average intensity $\bar{I}(\tau)$ also has the form of a pulse.

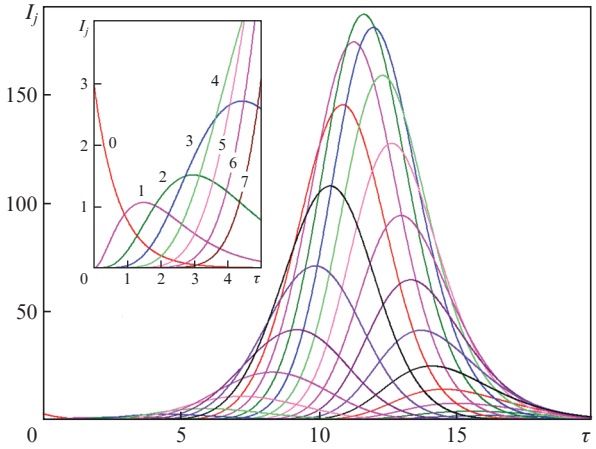

Figure 2. (Colour online) Time variation of the mode intensity I_j after the AOM was switched on at a time $\tau = 0$. The mode numbers are indicated at the curves. In the computations, we used $\kappa_\mathrm{d} = 0.5$ and $\delta\nu = 20$ kHz.

Partial overlap of pulses allows us to address locking of a relatively small number of modes. Figure 3 illustrates the effect of diffraction field injection on mode locking characteristics at $\delta\nu = 20$ kHz. The modal composition for the average intensity $\bar{I}(\tau)$ at the beginning of a pulse differs markedly from that at its end (this is consistent with the data in Fig. 2). In the beginning, a smaller number of modes with small j are locked, whereas in the end more modes with large j are locked. For this reason, individual mode-locked pulses, $\bar{I}(\tau)$, turn out to be shorter in the end. At $\kappa_\mathrm{d} = 0.5$ (Fig. 3a), the $\bar{I}(\tau)$ duration is approximately 10τ and the duration of individual mode-locked pulses is about 0.1τ.

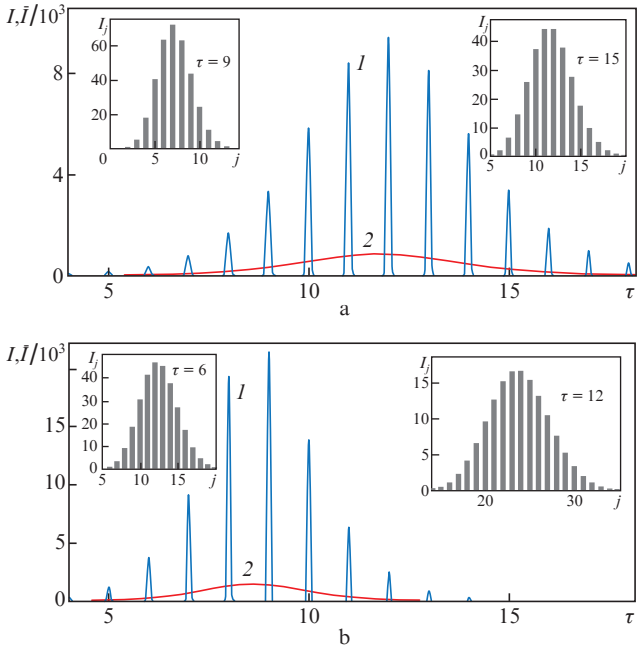

Figure 3. (*1*) Intensity I and (*2*) average intensity $\bar{I}$ as functions of time for external Q-switching at κ_d = (a) 0.5 and (b) 0.8. Insets: modal compositions of the laser radiation at different instants of time τ.

Increasing the diffraction coupling coefficient κ_d to 0.8 (Fig. 3b) causes a larger number of modes to be involved in lasing, the mode-locked pulse duration decreases, and the pulse height rises twofold (even though the diffraction loss rises with κ_d). At the same time, inversion drops more rapidly and the $\bar{I}(\tau)$ duration decreases to 5τ.

In the case of zero detuning ($\delta\nu = 0$), the phases of all modes remain equal to each other [$\varphi_j(\tau) = 0$] and, according to (2), the in-phase summation of mode fields occurs at time $\tau = \tau_m$, when $\psi_j(\tau_m) = 2\pi m$, where m is an integer. Since $m = j\tau_m$, τ_m should be an integer as well.

At $\delta\nu \neq 0$, the $\varphi_j(\tau)$ values are solutions to equations (1). The data presented in Fig. 4 demonstrate that the phase of each mode rises linearly with time, with a slope $\delta\nu/\delta\nu_c$. In this case, in-phase summation of mode fields occurs at $m = j\tau_m(1 + \delta\nu/\delta\nu_c)$. Therefore, τ_m is no longer an integer. At a relatively small detuning $\delta\nu$ (20 kHz) and $\tau_m \approx 10$, the ψ_j values for the first nine modes differ little (Fig. 4, left inset).

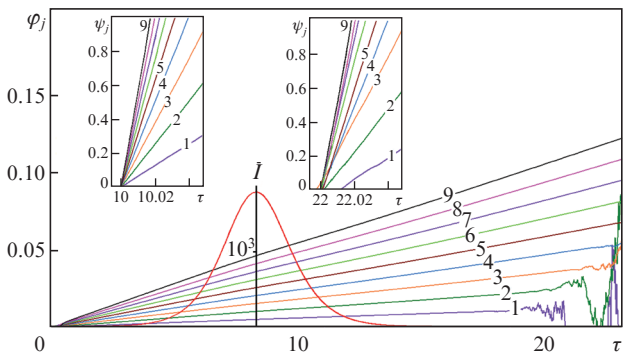

Figure 4. Mode phases φ_j, ψ_j functions and average intensity $\bar{I}$ vs. time after the AOM was switched on at time $\tau = 0$ at $\kappa_d = 0.8$ and $\delta\nu$ = 20 kHz. The mode numbers are indicated on the lines.

When the AOM is switched off, the laser has relatively low efficiency because the reflectivity of the mirror of the retroreflector, r_1, is relatively small. Even though energy efficiency is beyond the scope of this work, it is worth noting that, when the AOM is switched on, the energy output per unit volume of the gain medium is considerably higher because, in the loop containing the diffracted beam, the reflectivity of the mirror meets the relation $r_2 \gg r_1$. At a sufficiently high κ_d, a laser with an analogous loop operates at $r_1 = 0$ as well [13]. On the other hand, a low-finesse cavity has a considerable bandwidth, which may be comparable to the mode spacing. This suggests the feasibility of mode locking at a considerably higher $\delta\nu$ value. Calculations show that the mode-locked pulse amplitude does not decrease at $\delta\nu$ up to at least 300 kHz.

The rather large amplitude of $\bar{I}(\tau)$ pulses (the highest $\bar{I}$ exceeds the I_0 of steady-state lasing by approximately 600 times) leads to strong saturation of the medium, and the mode fields E_j decrease to the level of the spontaneous field (in Fig. 4, this occurs for $\tau > 20$). Note that, because of the stochasticity of spontaneous mode fields, the j values differ from each other at any τ (Fig. 4, right inset).

Subsequently (after the AOM is switched off), inversion returns to its original level and steady-state lasing on the $j = 0$ mode reappears. Effective periodic external Q-switching is possible with a period approaching the inversion recovery time T_1. Under such conditions, the number of locked modes is relatively small, so the pulse duration is shorter than the cavity round-trip time T_c by just about ten times. The rather large diffraction coefficient ($\kappa_d \approx 0.8$ and above) allows one to obtain peak pulse intensities about 10^4 times the steady-state lasing intensity on the fundamental mode.

4. Self-oscillation regime

As shown earlier [9, 10], steady-state lasing in such a system is unstable for a rather wide set of parameters, which leads to excitation of average intensity self-oscillation at a relaxation frequency. Self-oscillation characteristics for the set of parameters chosen are presented in Fig. 5.

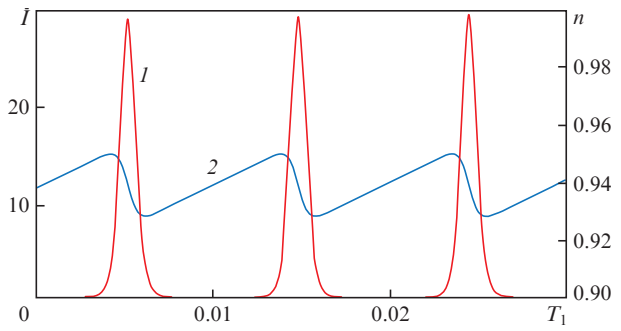

Figure 5. (*1*) Average intensity $\bar{I}$ and (*2*) inversion n as functions of time T_1 in the self-oscillation regime at $\kappa_d = 0.7$ and $\delta\nu$ = 30 kHz.

A distinctive feature of such a regime in the system under consideration is that lasing occurs at an inversion below threshold for any particular mode. This suggests that the self-oscillation regime is due to injection from a spontaneous emission level of the modes. All modes operate in the regenerative amplification regime. The pulse separation of steady-state self-oscillations is about a factor of 100 shorter than the

inversion recovery time T_1, so saturation of the medium is not very strong.

Figure 6 shows a pulse in the self-oscillation regime. Comparison of its parameters with those in the external Q-switching regime attests to a shift of the intensity to higher order modes (Fig. 6, inset) and an increase in the number of modes involved in lasing (~ 100). At the same time, the maximum value of $\bar{I}(\tau)$ decreased considerably and the pulse duration increased. The reason for this is that the growth of the fields is less effective because of the small injected field amplitudes in the case of low-order modes. As a result, high-order modes have an advantage. The medium saturates more slowly, which allows a larger number of modes to be involved in lasing. The rise in the number of modes leads to narrowing of ML pulses, whose absolute width becomes of the order of 10^{-10} s.

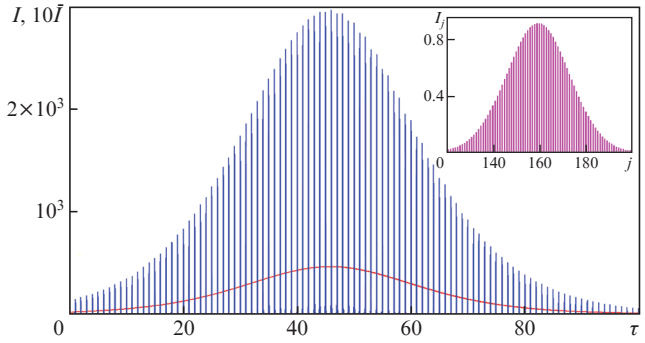

Figure 6. Mode-locked pulses and average intensity $\bar{I}$ (solid line) in the self-oscillation regime at $\kappa_d = 0.7$ and $\delta\nu = 30$ kHz. Inset: modal composition of the laser radiation.

Mode locking in the external Q-switching regime is possible because φ_j is a linear function of time. As a result, the condition for in-phase summation of mode fields is met periodically. Mode locking in the self-oscillation regime requires clarification. The field intensity between self-oscillation pulses can be comparable to the spontaneous field level and their phases φ_j can remain stochastic during the formation of a sequential self-oscillation. At the same time, calculations show that, after just $\sim 10^{-3}T_1$, the continuing field injection process gradually smoothens independent phase jumps of spontaneous emission in high-order modes because each mode 'imposes' its phase on the next one. This process becomes more active with increasing inversion. With increasing field intensity, field phases become regular and vary almost linearly with time.

Figure 7 illustrates the behaviour of the $\psi_j(\tau)$ functions for the ten strongest modes. The data in Figs 7a and 7b correspond to $\delta\nu = 40$ kHz, and the data in Fig. 7c, presented for comparison, correspond to $\delta\nu = 0$. The $\psi_j(\tau)$ functions are given at the instant roughly corresponding to the onset of a self-oscillation pulse (near $\tau = 0$ in Fig. 6). The arrows indicate the instant of in-phase field summation (when the mode-locked pulse has the largest amplitude). In-phase summation occurs periodically at an integer time τ_m (in units of T_c) and $\delta\nu = 0$ (Fig. 7c), whereas at $\delta\nu \neq 0$ the values of τ at such points are non-integers (Figs 7a, 7b). At these points, $\psi_j(\tau)$ lies in the interval $[0, 2\pi]$.

Comparison of Figs 7a and 7b demonstrates that the injection process plays an important role in 'imposing' the

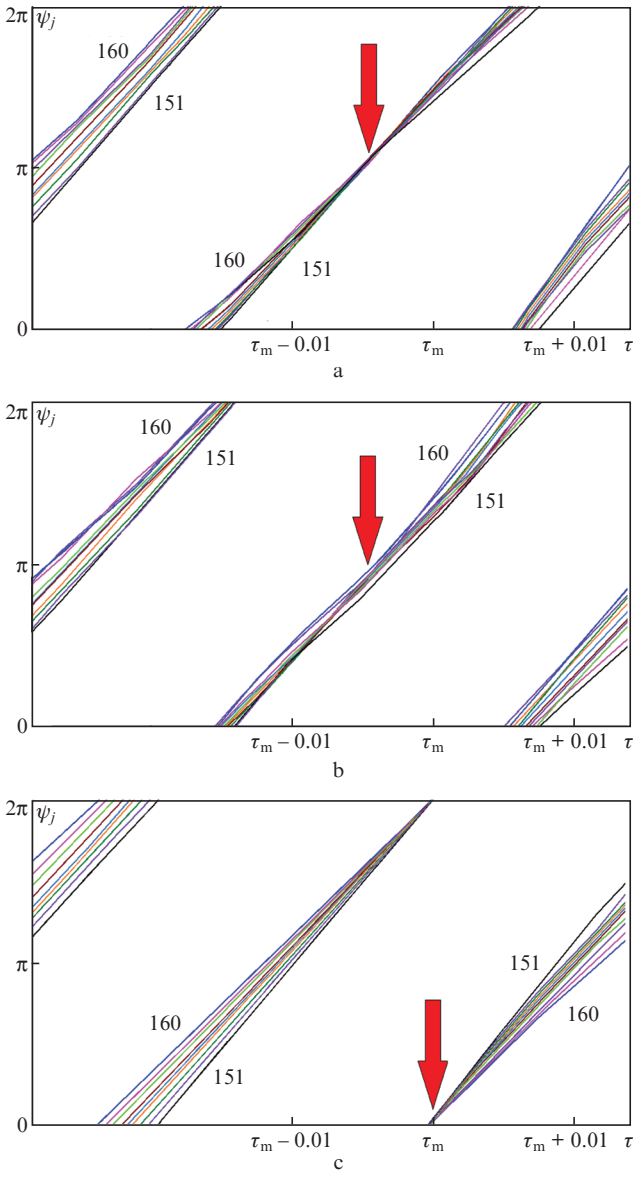

Figure 7. Behaviour of $\psi_j(\tau)$ in the self-oscillation regime: (a) $\kappa_d = 0.75$, $\delta\nu = 40$ kHz; (b) $\kappa_d = 0.4$, $\delta\nu = 40$ kHz; (c) $\kappa_d = 0.75$, $\delta\nu = 0$. The mode numbers are indicated at the lines; τ_m is an integer.

phase. Injection is much more effective at high κ_d values (Fig. 7a), owing to which the phases remain linear functions of time. At lower κ_d values, there are only approximate linear relations (Fig. 7b) and the fields are not completely in phase.

The effectiveness of the injection process in 'imposing' the phase enables mode locking in a wide range of $\delta\nu$ detuning values.

At the same time, $\delta\nu$ influences the dynamics of the mode fields involved in the formation of a self-oscillation pulse and, for this reason, it controls laser output characteristics. Interference of the injected field E_{j-1} with field E_j is determined by $\Phi_j = \varphi_{j-1} - \varphi_j + 2\pi\delta\nu T_c\tau$, which is zero at $\delta\nu = 0$. An increase in $\delta\nu$ leads to an unfavourable increase in Φ_j, slowing down the growth of weak fields between pulses. Because of this, intensity $\bar{I}$ rises only slowly, so the pulse separation increases, and every self-oscillation pulse appears at a higher inversion value. This is accompanied by an increase in average intensity $\bar{I}$ and, accordingly, in mode-locked pulse amplitude. Calcu-

lations show that increasing $\delta\nu$ from 30 to 300 kHz increases the $\bar{I}$ pulse separation to about $0.05T_1$ (cf. Fig. 5). Concurrently, $\bar{I}$ rises by an order of magnitude and the pulse duration drops to about 20τ. The peak intensity of the mode-locked pulses rises to $I = 1.5 \times 10^4$ (i. e. to a level attainable in the external Q-switching regime), and the modal composition shifts to lower j values. Thus, varying the detuning, one can control self-oscillation parameters.

5. Conclusions

We have proposed a numerical model for a laser with an AOM that ensures a frequency shift by almost half the mode spacing. Light is returned to the cavity by a retroreflector which has high reflectivity for the frequency-shifted light and low reflectivity for the unshifted light. The model takes into account field injection from a given mode to the next one and the stochasticity of the amplitude and phase of spontaneous emission. The model has been used to analyse the effect of field injection on the dynamics of QML lasing. In particular, it has been shown that the injection process helps to maintain a linear time variation of the phases of individual modes. At a large cavity bandwidth, this allows mode locking to be achieved at an appreciable frequency shift detuning from half the mode spacing. The laser is capable of operating in two modes. In one mode, the AOM is periodically switched on with a period typically near the inversion recovery time (external Q-switching). In the other, the system operates in the self-oscillation regime, with the AOM switched on throughout. The characteristics of both modes have their own distinctive physical features.

In the case of external Q-switching, the pulses have high intensity and a variable frequency composition, with a total duration of the order of ten cavity round-trip times ($\sim 10T_c$). During a pulse, the intensity of the fundamental mode drops rapidly and pulses at frequencies of about 20 higher order modes sequentially appear. With increasing diffraction coefficient, the number of locked modes increases. One advantage of this regime is the possibility of generating pulse trains with a high peak intensity and duration $\tau_p \sim 0.1T_c$.

The self-oscillation lasing regime is due to injection from a spontaneous emission level of the modes. A major contribution to the total intensity is made by high-order ($j > 100$) modes. Inversion does not reach threshold and all modes operate in the regenerative amplification regime. The number of locked modes in the self-oscillation regime is approximately ten times greater, which results in pulses of duration $\tau_p \sim 0.01T_c$ ($\tau_p \sim 10^{-10}$ s under our conditions), which are similar in peak intensity to those in the external Q-switching regime. Another distinctive feature of the self-oscillation regime is that its characteristics can be controlled by varying detuning $\delta\nu$. This is due to the effect of $\delta\nu$ on the relaxation frequency of the laser. An increase in $\delta\nu$ leads to a reduction in the rate of the increase in the mode fields between self-oscillation pulses, which allows inversion to be accumulated before the next pulse.

References

1. Zhang G., Jiao Z. *J. Mod. Opt.*, **65** (8), 994 (2017).
2. Tian W., Wang C., Wang G., Liu S., Liu J. *Laser Phys. Lett.*, **4**, 196 (2007).
3. Lin J., Chen H., Hsu H., Wei M., Lin K., Hsieh W. *Opt. Express*, **16**, 16538 (2008).
4. Han C., Zhao S., Li G., et al. *Laser Phys.*, **21**, 1769 (2011).
5. Zhang L., Wang Y.G., Yu H.J., et al. *Laser Phys.*, **21**, 454 (2011).
6. Zhang G., Zhao S., Zhao B., Wang Y. *Int. J. Appl. Phys. Math.*, **5**, 137 (2015).
7. Li T., Zhao S.Z., Zhuo Z., et al. *Opt. Express*, **18**, 10315 (2010).
8. Donin V.I., Yakovin D.V., Gribanov A.V. *Quantum Electron.*, **42**, 107 (2012) [*Kvantovaya Elektron.*, **42**, 107 (2012)].
9. Donin V.I., Yakovin D.V., Gribanov A.V. *JETP Lett.*, **101** (12), 783 (2015) [*Pis'ma Zh. Eksp. Teor. Phys.*, **101** (12), 881 (2015)].
10. Nanii O.E., Odintsov A.I., Panakov A.I., Smirnov A.P., Fedoseev A.I. *Quantum Electron.*, **47** (11), 1000 (2017) [*Kvantovaya Elektron.*, **47** (11), 1000 (2017)].
11. Kornienko L.S., Kravtsov N.V., Nanii O.E., Shelaev A.N. *Sov. J. Quantum Electron.*, **11** (12), 1557 (1981) [*Kvantovaya Elektron.*, **8** (12), 2552 (1981)].
12. Kasahara K., Nakamura K., Sato M., Ito H. *IEEE J. Quantum Electron.*, **34** (1), 190 (1998).
13. Stellpflug M., Bonnet G., Shore B.W., Bergmann K. *Opt. Express*, **11**, 2060 (2003).